SPACE WEATHER STUDY USING COMBINED CORONAGRAPHIC AND *IN SITU* OBSERVATIONS

N. Gopalswamy
Center for Solar Physics and Space Weather, The Catholic University of America, Washington DC 20064, and NASA/GSFC, Greenbelt, MD 20771, USA

ABSTRACT

Coronal mass ejections (CMEs) play an important role in space weather studies because of their ability to cause severe geoeffects, such as magnetic storms. Shocks driven by CMEs may also accelerate solar energetic particles. Prediction of the arrival of these CMEs is therefore of crucial importance for space weather applications. After a brief review of the prediction models currently available, a description of an empirical model to predict the 1 AU arrival CMEs is provided. This model was developed using two-point measurements: (i) the initial speeds and onset times of Earth-directed CMEs obtained by white-light coronagraphs, and (ii) the corresponding interplanetary CME speeds and onset times at 1 AU obtained *in situ*. The measurements yield an empirical relationship between the interplanetary acceleration faced by the CMEs and their initial speeds, which forms the basis of the model. Use of archival data from spacecraft in quadrature is shown to refine the acceleration versus initial speed relationship, and hence the prediction model. A brief discussion on obtaining the 1-AU speed of CMEs from their initial speeds is provided. Possible improvements to the prediction model are also suggested.

INTRODUCTION

Space Weather conditions are primarily driven by the activity on the Sun, directly related to the evolution of open and closed magnetic fields. The open magnetic fields carry high speed solar wind while solar eruptions occur in closed magnetic field regions, such as active regions, filament regions or a combination thereof. Apart from electromagnetic radiation, which reaches Earth in minutes, solar eruptions result in three propagating entities that may affect the near-Earth space environment: coronal mass ejections (CMEs) (observed in the solar wind as magnetized plasma ejecta), solar energetic particles (SEPs), and interplanetary (IP) shocks. These entities are not independent: Fast mode shocks are driven by solar ejecta and the shocks in turn accelerate SEPs. A class of IP shocks have been observed without obvious drivers behind them (Schwenn, 1996) but we now know that these shocks are driven by CMEs (Gopalswamy et al. 2001a) traveling perpendicular to the Sun-Earth line. Short-lived SEPs can also result from solar flares without accompanying mass ejections (see, e.g., Reames 1996 for a review). For space weather applications, one should be able to predict quantitative information, such as the time of arrival. It is well known that the SEPs typically arrive within an hour after their injection near the Sun and that it is very difficult to predict their onset. More important are the particles that arrive along with the IP shock, commonly referred to as "energetic storm particles" or ESPs. These "shock enhancements" could be up to two orders of magnitude larger in flux and hence pose a hazard to astronauts and space-based technological systems. Thus, prediction of the arrival of IP shocks in the vicinity of Earth is a crucial element in space weather research. Since there is a definite relationship between CMEs and IP shocks (see, e.g., Sheeley et al., 1985), prediction of one of them should be often sufficient. In this paper, we review some of the current efforts in predicting the arrival of CMEs at 1 AU based on remote sensing while the CMEs are still near the Sun.

CURRENT MODELS

It was recognized long ago that IP shocks are one of the earliest signatures of solar disturbances and have been extensively studied from the point of view of geoeffects (Chao and Lepping, 1974; Russell et al., 1983; Marsden et al., 1987; Lindsay et al., 1994). Although it was recognized early on that most of the IP shocks were associated with white-light CMEs (Sheeley et al., 1985), the initial attempts to predict the arrival of IP shocks were not based on CMEs: The Shock Time Of Arrival (STOA) model (see, e.g., Smart and Shea 1985) and the Interplanetary Shock Propagation Model (ISPM, Smith and Dryer, 1990). Both of these models use observations of metric type II bursts as the primary source of input. Metric type II bursts indicate shocks in the inner corona. The shock speed is estimated from the drift rate of type II bursts assuming a density model for the corona. Propagation of these coronal shocks through the IP medium is studied in order to predict their arrival time and strength at 1 AU.

In the STOA model, a flare explosion drives a shock which propagates initially at a constant speed, followed by a deceleration of the blast wave. The shock propagates quasi-spherically through a radially-variable solar wind, centered at the flare site. The shock is assumed to be perpendicular and driven for the duration of the flare. It is also assumed that the events are sufficiently far apart that there is no shock interaction in the IP medium. The ISPM uses the same inputs as the STOA model, but assumes an upper cut-off of two hours for the flare duration.

There are a few basic problems with these models. First, observations do not seem to support the predictions of these models. It was pointed out by Gopalswamy et al. (1998a) that there was very little correspondence between coronal shocks inferred from metric type II bursts and the IP shocks detected *in situ* over a period of 18 months. In a more comprehensive study, Gopalswamy et al. (2001a) compared 137 metric type II bursts and 49 IP events (ejecta and IP shocks) that occurred during November 1994 to June 1998. They looked for 1 AU counterparts of a subset of 44 coronal shocks inferred from on-disk metric type II bursts and solar counterparts of IP events. The reason for using on-disk type II bursts is that these are the events that are likely to have near-Earth signatures. Imposing the constraint that near-Sun and near-Earth manifestations should have corresponding signatures within 5 days, they found that (i) most (93 %) of the metric type II bursts did not have IP signatures and (ii) most (80 %) of the IP events (IP ejecta and shocks) did not have metric counterparts. Kadinsky-Cade et al. (1998) and Quigley and Kadinsky-Cade (2000) have accumulated a huge data base of metric type II bursts and flares for testing the STOA model and ISPM. Their initial finding was that the "results are disappointing". Second, these models have an inner computational boundary at 18 solar radii ($R_\odot$). Between the solar surface and 18 $R_\odot$, the corona changes its structure rapidly and the radial profiles of physical quantities are not uniform. One of the most important parameters that determines shock propagation is the speed profile of the fast mode. This speed starts at a value as small as 200 km s^{-1} at the coronal base and attains a peak value of > 500 km s^{-1} around 3 $R_\odot$. This radial profile of the fast mode speed may act as a filter because shocks with speeds less than this peak fast mode speed may not propagate past this hump (see Mann et al., 1999; Gopalswamy et al., 2001a). Furthermore, slow but accelerating CMEs with no metric radio burst signature can also produce IP shocks at distances beyond the speed hump. Finally, the assumption of perpendicular propagation is not consistent with all the CME-driven IP shocks. Recently, Berdichevsky et al. (2000) found that only a little more than half of the IP shocks are quasi-perpendicular; the rest is oblique or quasi-parallel.

The poor correlation between metric type II bursts and IP shocks does not support the numerical models (STOA model and ISPM). The small fraction of metric type II bursts that did have IP association invariably involved large-scale CMEs. Coupled with the fact that most of the IP shocks are associated with large-scale CMEs (Sheeley et al., 1985) one can conclude that CME is the primary near-Sun activity that significantly disturbs the solar wind in the vicinity of Earth (see also Gosling, 1993). Therefore, CME-based space weather prediction methods are likely to be more realistic. It must be pointed out that this paper deals only with the arrival of CMEs at 1 AU and it is straight forward to predict the arrival of IP shocks based on the known relationship between a shock and its driving CME.

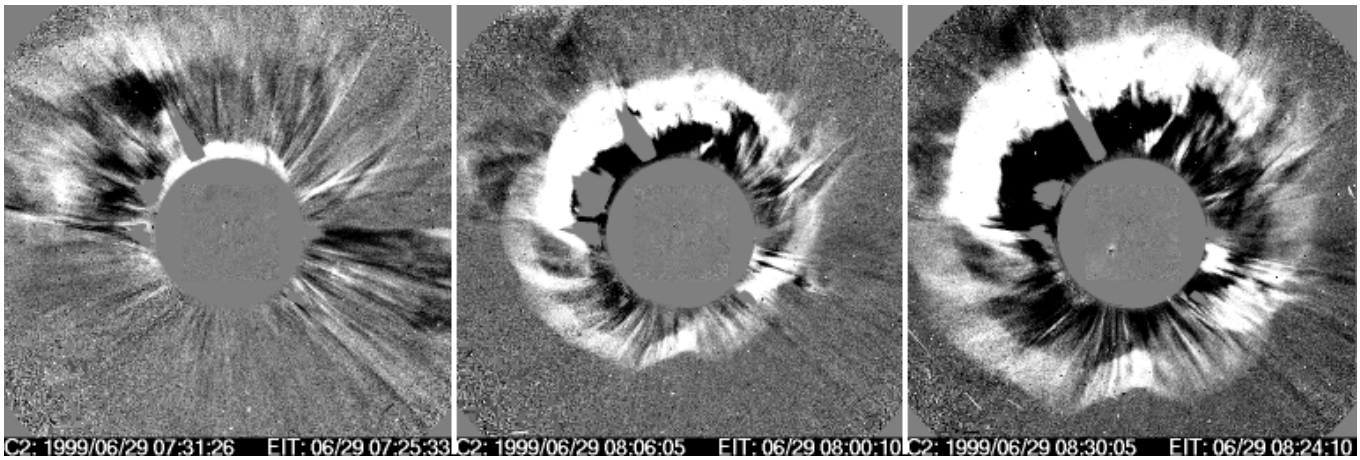

Figure 1: A near-perfect halo CME heading in the anti-Earthward direction shown in three SOHO/LASCO C2 difference images. The CME can be seen appearing above the occulting disk in the first image at 07:31 UT. In the second image at 08:06 UT, the CME has completely surrounded the occulting disk (the circular disk). SOHO/EIT difference images are superposed on SOHO/LASCO images. No changes can be seen on the disk, except for a tiny change seen in the last image at 08:30 UT by which time the CME has moved close to the edge of the LASCO field of view and hence unrelated. The CME was moving with a sky plane speed of about 630 km s^{-1}. The eruption must have occurred on the backside of the Sun.

HALO CMEs AND GEOEFFECTS

The term "halo CME" refers to a transient enhancement in the white light corona that appears to completely surround the occulting disk of a coronagraph (Howard et al., 1982). Because of the unfavorable conditions presented by halo CMEs to be detected by Thomson-scattered photospheric light (see Michels et al., 1997 for a detailed discussion), many of the halo CMEs are not very obvious. White light observations cannot show whether a halo CME is moving in the earthward or anti-Earthward direction. We need observations from inner coronal imagers such as SOHO/EIT or Yohkoh/SXT to identify the source of the eruption. Ground-based observations in Hα or microwaves can also tell us something about disk activities associated with CMEs (Gopalswamy, 1999). An anti-Earthward halo CME would not have a disk signature. Fig. 1 shows a spectacular halo event that occurred on June 29, 1999 which did not have a disk signature ("backside event"). This event was recorded by the Large Angle and Spectrometric Coronagraph (LASCO) onboard SOHO. The images are shown in running difference so the dark regions represent the location of the CME in the previous frame. Fig. 2 shows the famous "Bastille day" event (July 14, 2000). This was a frontside halo as evidenced from the EUV eruption near the disk center. These are two examples of a large number of halo CME events routinely observed by the SOHO coronagraphs. These observations have put halo CMEs in the spotlight and they are being explored as harbingers of geomagnetic storms.

Brueckner et al. (1998) examined the correlation between a set of eight halo CMEs and found that the geomagnetic storms followed the halo CMEs after about 80 hours. As these authors pointed out, the arrival time may not apply to fast events and to those occurring during the rising phase of the current solar cycle. Watari and Watanabe (1999) selected 52 geomagnetic storms with Dst < -50 nT during the same period as Brueckner et al. (1998) and identified the solar sources of these storms using Yohkoh soft X-ray data. They found that about half of the geomagnetic storms were associated with interplanetary CMEs (ICMEs) while the other half were associated with high speed streams. They also found that about 75 % of magnetic clouds were associated with geomagnetic storms. Webb et al. (2000) considered a set of seven halo CMEs and their terrestrial consequences and found that all of them were associated with magnetic clouds and geomagnetic storms. Gopalswamy et al. (2000a) studied a larger sample – a set of 23 interplanetary ejecta detected *in situ* by the Wind spacecraft – and identified the associated white-light events. They eliminated limb and backside events using optical, X-ray and EUV images and established that most of the IP ejecta

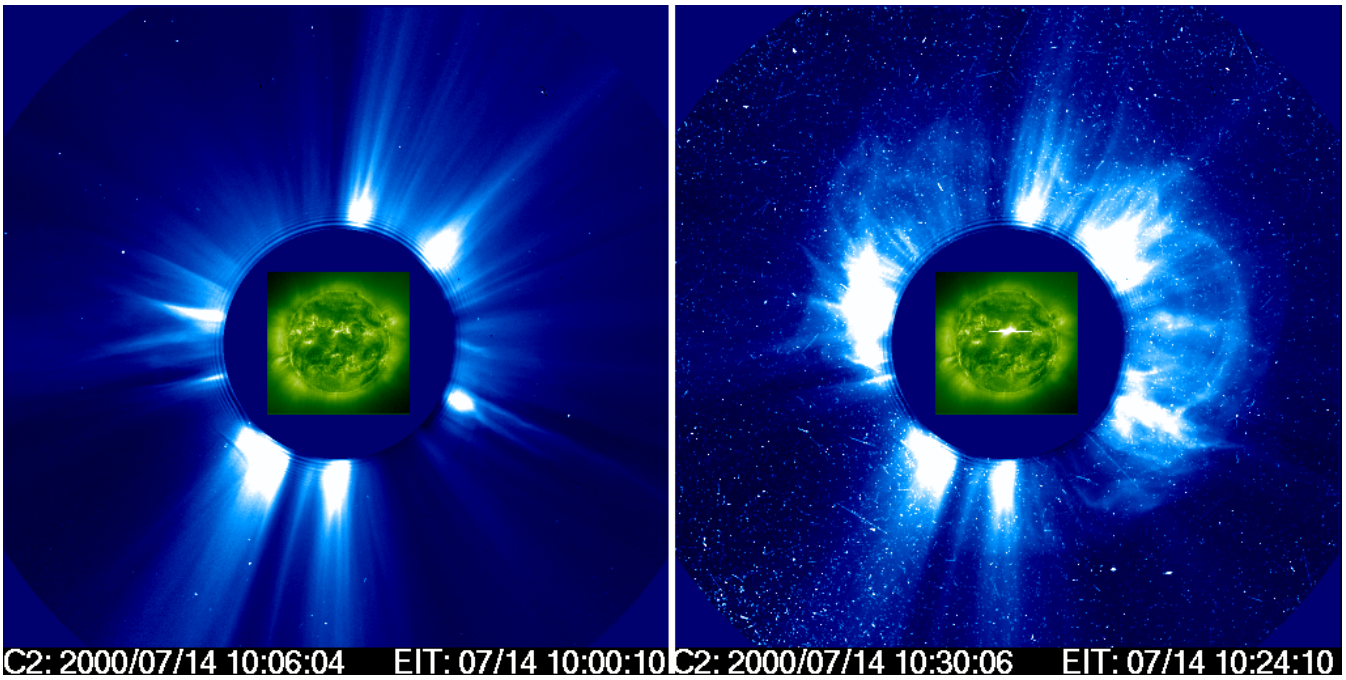

Figure 2: An Earth-directed CME that occurred on July 14, 2000 (known as the 'Bastille Day event'). EIT images (at 10:00 and 10:24 UT) are superposed on the SOHO/LASCO C2 images (at 10:06 and 10:30 UT). A bright eruption can be seen in the EIT image at 10:24 UT which is associated with the halo CME seen at 10:30 UT surrounding the occulting disk. The "snow storm" background in the right panel is due to SEPs hitting the SOHO detectors.

were associated with solar eruptions that occurred near the disk center (average latitude of 17° and average longitudinal distance of 27°). Recently, St Cyr et al. (2000) studied the annual and cumulative statistics for Kp index in comparison with halo CME events observed by SOHO. They considered 21 geomagnetic storms (Kp indices ≥ 6) that occurred during a 25 month period (January 1996 to June 1998, similar to the period of Gopalswamy et al., 2001a) and found that 15/21 (71 %) of the storms were associated with frontside halo CME events. Thus, frontside halo CMEs account for a major fraction of geomagnetic storms and need to be studied for prediction purposes. In the following, we discuss how we can predict the arrival of CMEs at 1 AU based on remote sensing of frontside halo CMEs.

AN EMPIRICAL CME ARRIVAL MODEL

Based on a set of IP ejecta detected *in situ* by Wind and the corresponding earthward CMEs detected by SOHO, Gopalswamy et al. (2000a) developed an empirical model to predict the arrival of CMEs at 1 AU. The IP ejecta had speeds in the range 350 - 650 km s^{-1} as measured *in situ*, compared with the corresponding white light CMEs, which had speeds in the range 150 - 1050 km s^{-1}. Gopalswamy et al. (2000a) set out to quantify the striking observation that the ICME-speed distribution was much narrower than the CME-speed distribution. They postulated that a CME undergoes an effective acceleration as it propagates through the IP medium and arrives at 1 AU with a different speed, assuming that they were observing the same CME at two different instances, without considering the internal structure of the CMEs. Although the exact relation between CMEs and their interplanetary counter parts (ICMEs) are not fully understood, one may expect that the spatial structure of a CME observed near the Sun is preserved as it propagates through the IP medium to produce the temporal structure observed *in situ*. For example, the ordering of substructures near the Sun (shock, frontal structure, cavity and prominence core) and at 1 AU (shock, sheath, IP ejecta and pressure pulse) may be preserved at least in some cases (Gopalswamy et al., 1998b).

Theoretically, one has to consider the resultant of the propelling and damping forces that act on the CME in order to study the dynamics of the CME through the IP medium (see, e.g., Chen, 1997). Observationally, we have only two measurements of the CME, one near the Sun performed remotely (using white light coronagraphs, such as SOHO/LASCO) and the other locally (using *in situ* plasma and magnetic field detectors, such as those onboard Wind). The effective acceleration is an average quantity, because CMEs near the Sun may show acceleration, constant speeds or even deceleration (Gopalswamy et al., 2001c). The onset time near the Sun for CMEs and the onset time for the ICMEs at 1 AU are known, so one can get the transit time, τ, for the CMEs. The respective coronagraphic and *in situ* measurements give the final and initial speeds of the CME at the two spatial points. The difference between the initial and final speeds, $\delta v = v - -u$, when divided by τ gives the effective acceleration ($a = \delta v/\tau$) for each of the CMEs.

It was found that the effective acceleration and the CME initial speeds were highly correlated (correlation coefficient = 0.98). A straight-line fit to the data points yielded an empirical relation between the acceleration (a) and initial speed (u) of the CME: a = 1.41 - 0.0035 u (a and u are in units if (m s^{-2}) and km s^{-1}, respectively). This relation was then used in the kinematic relation, $S = ut + 1/2\ a\ t^2$ (where S = Sun-Earth distance (1 AU)) to predict the *arrival time, t,* of CMEs at 1 AU. The only input parameter in this model is the initial CME speed and thus provides a simple means of advance warning of solar disturbances arriving in the vicinity of Earth. Of course, we need the background information, such as disk signatures to confirm that the halo CMEs are frontside events and their location to be close to the central meridian. The all-important initial speed of the CME needs to be measured accurately to get a reliable arrival time prediction.

An Earth-directed halo CME appears to spread in the sky plane and what we measure is this spreading speed. This may or may not be the true speed of the CME. The CMEs are detected in the photospheric light Thomson-scattered by coronal material. Material in the plane of the sky is best observed by this process, so the measured speed of halo CMEs are subject to projection effects. Gopalswamy et al. (2000b) found a definite correlation between the CME speeds and the central meridian distance, with the fastest events coming from the limb. Therefore, as pointed out by Gopalswamy et al. (2000a), the empirical CME arrival model has the problem of projection effects. In order to overcome this projection effect, one needs to have stereoscopic observation, to be available in the future from the STEREO mission. However, there were some archival observations free from projection effects, which we describe below (see also Gopalswamy et al., 2001c for more details).

IMPROVING THE CME ARRIVAL MODEL

Sheeley et al. (1985) studied a large number of IP shocks detected *in situ* by the Helios-1 spacecraft and were able to identify a corresponding white light CME near the Sun using the Solwind coronagraph on board the P78-1 spacecraft (Doschek, 1983). A large fraction of these IP shocks were followed by pistons, the IP manifestations of the white light CMEs. For all these events, P78-1 was located along the Sun-Earth line while the Helios-1 spacecraft was located above east or west limb of the Sun. Thus two spacecraft were observing the same event in quadrature so that the remote sensing and local sensing corresponded to the same part (nose) of the CME. The effective acceleration derived from these observations is devoid of projection effects. Although Helios-1 was not in the vicinity of Earth, it was possible to choose events for which Helios-1 was at a distance more than 0.7 AU, similar to the Sun-Earth distance. Lindsay et al. (1999) expanded the list of such events by including data from Pioneer Venus Orbiter (PVO) which was in quadrature with either P78-1 or the Solar Maximum Mission (SMM). They found a weak correlation between the ICME and CME speeds ($v = 0.25u$ + 360 km s^{-1}). This was one of the earliest attempts to link the near-Sun events to the corresponding ones in the IP medium. Gopalswamy et al (2001c) revised the list of Lindsay et al. (1999) eliminating uncertain events and came up with a set of 19 CME-ICME pairs observed by the Solwind coronagraph (remote sensing) and by PVO or Helios-1 (local sensing). When the analysis was repeated as in the case of SOHO/Wind events, the empirical relation between the effective acceleration (a) and initial speed (u) maintained the same functional form (a = 1.765 - 0.00429 u), thus confirming the original method of Gopalswamy et al. (2000a).

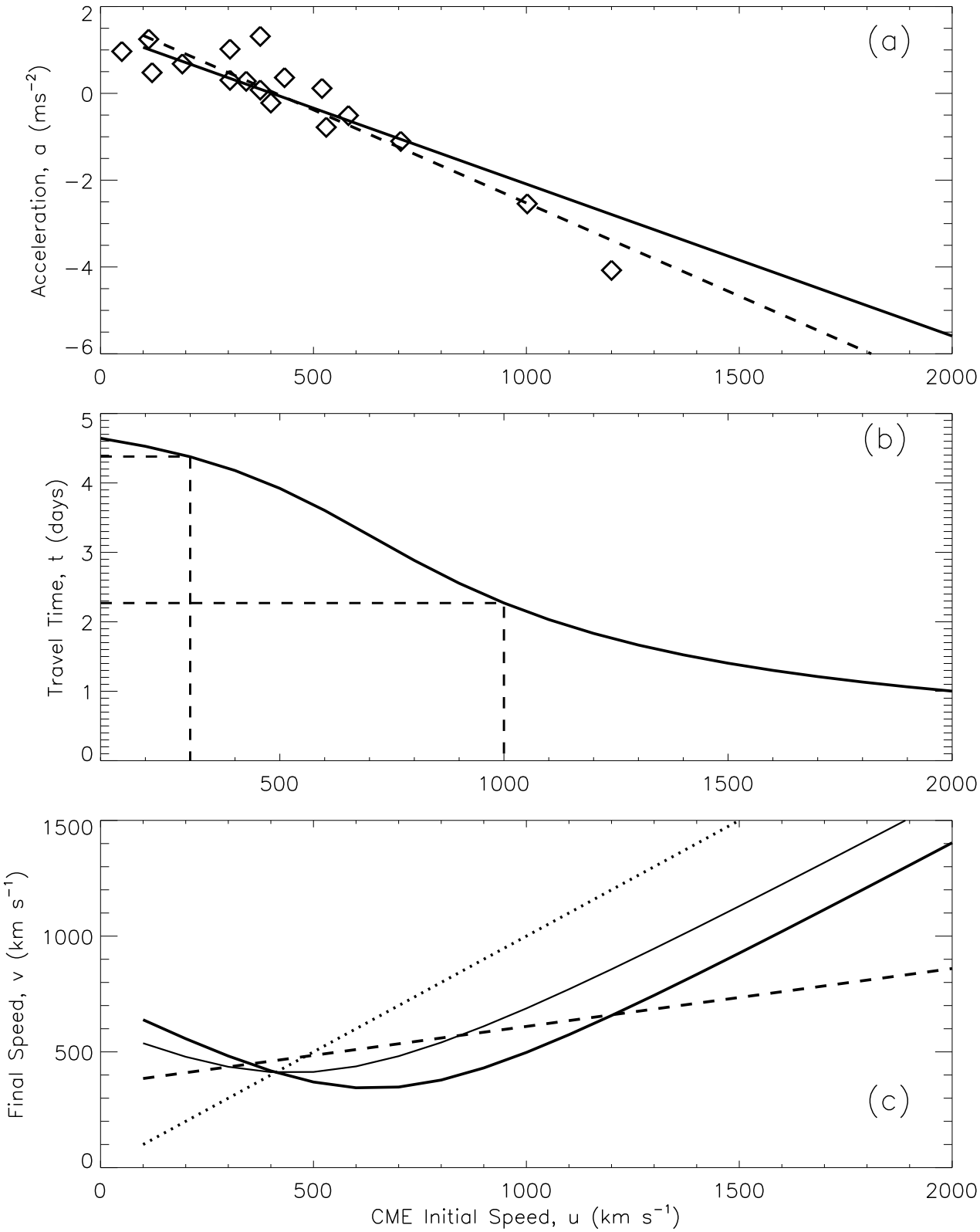

Figure 3: (a) Best-fit lines to the acceleration vs. initial speed plots for the SOHO/Wind (solid line) and Helios1-PVO/P78-1 CMEs (dashed line, fit to the data points shown by diamonds). (b) Prediction curve using accelerations derived from Helios1-PVO/P78-1 data. Note that a 200 km s^{-1} CME would arrive in 4.5 days while a 1000 km s^{-1} CME would take just over two days to arrive at 1 AU (see the dashed lines). (c) Final speeds of CMEs predicted from initial speeds based on no acceleration (dotted line), Lindsay et al. (1999 – dashed line) and Gopalswamy et al. (2001a – thick curve for $S = 1$ AU and thin curve for $S = 0.7$ AU).

The effective acceleration obtained from the SOHO/Wind and Helios1-PVO/P78-1 pairs is plotted in Fig. 3 (a) which shows that there is a significant deviation at low speeds. The solution of the kinematic equation with the new acceleration yielded a prediction curve as shown in Fig. 3 (b), very similar to the original curve in Gopalswamy et al. (2000a). The arrival time of low-initial speed SOHO CMEs is longer than what is seen in this curve because SOHO/LASCO underestimates the speeds of the slow CMEs and hence the model overestimates the arrival time (see Gopalswamy et al., 2000a). The prediction curve provides a simple way to estimate the arrival time of CMEs at 1 AU, once the initial speed of the Earth-directed CME is known from coronagraphic observations. Typical travel times for slow (300 km s^{-1}) and fast (1000 km s^{-1}) CMEs are shown by dashed lines as 4.4 and 2.3 days, respectively. If the IP medium had no influence, the corresponding travel times would be 5.7 and 1.7 days. The archival data and the SOHO/Wind data correspond to different phases of the solar cycle, yet the results are quite consistent. The archival data had events anywhere between 0.7 and 1 AU and the corresponding uncertainty introduced in the acceleration was ignored.

Since the ram pressure change in the solar wind impinging on the magnetosphere is important in determining the extent of geomagnetic disturbances, it is instructive to predict the final speed (v) of CMEs based on their initial speed (u). This was first attempted by Lindsay et al. (1999), who arrived at an empirical relation, $v = 0.25\ u + 360$ km s^{-1} as a straight line fit to the scatter plot of CME and ICME speeds. The final speed based can also be obtained using the acceleration model in the kinematic relation, $v^2 = u^2 + 2.a\ S$ as shown in Fig. 3 (c) along with the straight line obtained by Lindsay et al. (1999). The thin and thick parabolic curves correspond to final speeds at $S = 0.7$ and $S = 1$ AU, respectively. Although the linear and parabolic curves deviate from each other at low and high speeds, both are clearly far different from the zero-acceleration case (dotted curve).

FUTURE PROSPECTS

The simple empirical model discussed above should be improved in a number of ways. The following effects need to be considered:

1) When we compared the CME speeds near the Sun and at 1 AU, we did not explicitly consider the speed of the background solar wind. If we assume that the drag acting on the CMEs is similar to the aerodynamic drag (Cargill et al., 1995), it would depend on the ambient density and flow speed. In the equatorial plane, the solar wind does not pick up for several solar radii, and the ambient density is high, resulting in a large drag force. Thus one would expect a significant drag initially. In those regions where the solar wind speed has attained a steady value, the drag would be less for a given CME speed. If a CME is launched into a region of high solar wind speed, then the drag is expected to be smaller and the CME would arrive earlier at 1 AU.

2) A similar situation arises when CMEs are launched in quick succession from the same source region. The resulting drag would depend on the speed and density of the post-CME flow of the preceding CME.

3) CMEs can interact and get deflected from the Sun-Earth line or can merge with one another (CME cannibalism – Gopalswamy et al., 2001b). The CME cannibalism is more important for solar maximum conditions because of the enhanced CME occurrence rate. The net result is that the remote sensing and local sensing would yield different counts for CMEs. One has to give careful consideration to effects like these so that false alarms can be minimized.

4) It is necessary to understand the acceleration profiles of CMEs near the Sun. There are examples of acceleration, deceleration as well as constant speed near the Sun. Current remote sensing provides data out to 30 $R_\odot$ from the Sun while local sensing is done close to 1 AU. When data points become available for other distances, we will be able to obtain a better profile for the acceleration. The acceleration profile should also consider the possibility that the IP acceleration is not constant throughout the IP medium. For example an accelerating slow CME might stop accelerating when it attains the speed of the background solar wind. The interplanetary scintillation (IPS) technique can be used to extend the height-time history of CMEs over $\sim$ 1 AU using multiple radio sources, although it is not clear as to what part of the CME (or the CME-driven shock) is sensed by this technique.

5) Since almost all the interplanetary transient shocks are driven by CMEs, we can extend the CME arrival time to predict the arrival of IP shocks. This can be done based on the fact that there is a definite relation between the stand-off distance of the shock and the properties of the CME piston. Such a shock prediction scheme will also be useful for a better comparison with other shock arrival models.

SUMMARY

Attempts to predict the influence of large-scale Earth directed CMEs are in the beginning stages, but seem to be headed in the right direction. The most important parameter for this purpose is the initial CME speed. However, this is the most difficult parameter to measure for halo CMEs because of the nature of coronagraphic observations. Using a spacecraft located on the Sun-Earth line (to identify disk events) and another one at right angles to the Sun-Earth line (to measure the nose-speed of CMEs) seems to be the simplest way to measure the CME initial speed accurately. If ground based observations are able to identify the disk signatures, one spacecraft at right angles to the Sun-Earth line should be able to do the job. As for the effective acceleration, a two-point measurement is clearly inadequate. Measurements at several points between Sun and Earth are required to arrive at a realistic acceleration profile of CMEs. Ground based IPS observations may be used to provide a rough estimate if CMEs and radio sources are chosen carefully. A better understanding of how various substructures of the CME observed near the Sun evolve into the substructures of ICME would also help to obtain better acceleration profiles. Shock arrival times can be derived from the CME arrival times based on statistical results or theoretical considerations. The earlier models such as STOA and ISPM can also be modified by replacing the metric type II burst aspects with CME data and by moving the computational boundary closer to the Sun.

ACKNOWLEDGEMENTS

This research was supported by NASA, NSF and AFOSR. The author thanks Seiji Yashiro for help with the figures and Thomas Moran for comments on the manuscript.

REFERENCES

Berdichevsky, D., A. Szabo, R. P. Lepping, A. Vinas, and F. Marini, Interplanetary fast shocks and associated drivers observed through the 23rd solar minimum by Wind over its first 2.5 years, *J. Geophys. Res.*, 105, 27,289, (2000).

Brueckner, G. E., J. P. Delaboudiniere, R. A. Howard, S. E. Paswaters, O. C. St. Cyr, et al., Geomagnetic storms caused by coronal mass ejections (CMEs): March 1996 through June 1997, *Geophys. Res. Lett.*, 25, 3019, (1998).

Cargill, P. J., J. Chen, D. S. Spicer, and S. T. Zalesak, Geometry of interplanetary magnetic clouds, *Geophys. Res. Lett.*, 22, 647, (1995).

Chen, J., Coronal Mass Ejections: Causes and Consequences, A theoretical Review, in *Coronal Mass Ejections*, ed. N. Crooker, J. Joslyn, and J. Feynman, AGU monograph 99, p. 65, (1997)

Chao, J. K. and R. P. Lepping, A correlative study of ssc's interplanetary shocks, and solar activity, *J. Geophys. Res.*, 79, 1799, (1974).

Doschek, G. A., Solar instruments on the P78-1 spacecraft, *Solar Phys.*, 86, 9, (1983).

Gopalswamy, N., X-ray and Microwave signatures of Coronal Mass Ejections, in *Solar Physics with Radio Observations*, ed. T. Bastian, N. Gopalswamy and K. Shibasaki, *NRO Report* 479, Nobeyama Radio Observatory, p. 141, (1999).

Gopalswamy, N., M. L. Kaiser, R. P. Lepping, S. W. Kahler, K. Ogilvie, et al., Origin of coronal and interplanetary shocks - A new look with WIND spacecraft data, *J. Geophys. Res.*, 103, 307, (1998a).

Gopalswamy, N., Y. Hanaoka, T. Kosugi, R. P. Lepping, J. T. Steinberg, et al., *Geophys. Res. Lett.*, 25, 2485, (1998b).

Gopalswamy, N., A. Lara, R. P. Lepping, M. L. Kaiser, et al., Interplanetary Acceleration of Coronal Mass Ejections, *Geophys. Res. Lett.*, 27, 145, (2000a).

Gopalswamy, N., M. L. Kaiser, B. J. Thompson, L. Burlaga, A. Szabo, et al., Radio-rich Solar Eruptive Events, *Geophys. Res. Lett.*, 27, 1427, (2000b).

Gopalswamy, N., A. Lara, M. L. Kaiser, and J.-L. Bougeret, Near-Sun and near-Earth manifestations of solar eruptions, *J. Geophys. Res.*, in press, (2001a).

Gopalswamy, N., S. Yashiro, M. L. Kaiser, R. A. Howard and J.-L. Bougeret, Radio Signatures of Coronal Mass Ejection Interaction: Coronal Mass Ejection Cannibalism? *Astrophys. J.*, 548, L91, (2001b).

Gopalswamy, N., A. Lara, S. Yashiro, M. L. Kaiser and R. A. Howard, Predicting the 1-AU Arrival Times of Coronal Mass Ejections, *J. Geophys. Res.*, in press, (2001c).

Gosling, J. T., The solar flare myth, *J. Geophys. Res.*, 98, 18,937, (1993).

Howard, R. A., D. J. Michels, N. R. Sheeley, Jr., and M. J. Koomen, The observations of a coronal transient directed at Earth, *Astrophys. J.*, 90, 8173, (1982).

Kadinsky-Cade, K., S. Quigley, and G. Ginet, Validation of interplanetary shock propagation models, EOS TRANSACTIONS, 79(45), F712, (1998).

Lindsay, G. M., C. T. Russell, J. G. Luhmann, and P. Gazis, *J. Geophys. Res.*, 99, 11, (1994)

Lindsay, G. M., J. G. Luhmann, C. T. Russell, and J. T. Gosling, Relationships between coronal mass ejection speeds from coronagraph images and interplanetary characteristics of associated interplanetary coronal mass ejections, *J. Geophys. Res.*, 104, 12,515, (1999).

Mann, G., H. Aurass, A. Klassen, C. Estel, and B. J. Thompson, Coronal transient waves and coronal shock waves, in *Plasma Dynamics and Diagnostics in the Solar Transition Region and Corona*, ed. J.-C. Vial and B. Kaldeich-Schurmann, *ESA SP-446*, 477, (1999).

Marsden, R. G., T. R. Sanderson, C. Tranquille, K.-P. Wenzel, and E. J. Smith, ISEE 3 observations of low-energy proton bidirectional events and their relation to isolated interplanetary magnetic structures, *J. Geophys. Res.*, 92, 11,009, (1987).

Michels, D. J., R. A. Howard, M. J. Koomen, S. P. Plunkett, G. E. Brueckner, et al., Visibility of Earth-Directed Coronal Mass Ejections, in *Proc, Fifth SOHO Workshop*, Eur. Space Agency Publ., *ESA SP* 404, 567, (1997).

Quigley, S. and K. Kadinsky-Cade, Final Validation Results and Databases for two Solar-event Initiated Interplanetary Shock Propagation Models, in First S-RAMP Conference, Paper S1-P21, (2000).

Reames, D. V., Energetic Particles from Solar Flares and Coronal Mass Ejections, in *High Energy Solar Flares*, ed. R. Ramaty, N. Mandzhavidze, and X.-M. Hua, *AIP Conf. Proc.* 374, 35, (1996).

Russell, C. T., M. M. Mellott, E. J. Smith, and J. H. King, Multiple spacecraft observations of interplanetary shocks Four spacecraft determination of shock normals, *J. Geophys. Res.*, 88, 4739, (1983).

Schwenn, R., An Essay on Terminology, Myths and Known Facts: Solar Transient - Flare - CME - Driver Gas - Piston - BDE - Magnetic Cloud - Shock Wave - Geomagnetic Storm, *Astrophys. Space Sci.*, 243, 187, (1996).

Sheeley, N. R., R. A. Howard, M. J. Koomen, D. J. Michels, R. Schwenn, et al., *Astrophys. J.*, 484, 472, (1985).

Smart, D. F. and M. A. Shea, A simplified model for timing the arrival of solar flare-initiated shocks, *J. Geophys. Res.*, 90, 183, (1985).

Smith, Z. and M. Dryer, MHD study of temporal and spatial evolution of simulated interplanetary shocks in the ecliptic plane within 1 AU, *Solar Phys.*, 129, 387, (1990).

St. Cyr, O. C., R. A. Howard, N. R. Sheeley, Jr., S. P. Plunkett, Properties of coronal mass ejections: SOHO LASCO observations from January 1996 to June 1998 et al., *J. Geophys. Res.*, 105, A8, 18169, (2000).

Watari, S. and T. Watanabe, Interplanetary Disturbances Around the Solar Minimum of Cycle 22 in *Solar Wind Nine*, ed. S. R. Habbal, R. Esser, J. V. Hollweg, and P. A. Isenberg, p.733, (1999).

Webb, D. F., E. W. Cliver, N. U. Crooker, O. C. St. Cyr, and B. J. Thompson, Relationship of halo coronal mass ejections, magnetic clouds, and magnetic storms, *J. Geophys. Res.*, 7491, (2000).